Drug Design, Development and Therapy

Dovepress
open access to scientific and medical research

Open Access Full Text Article

ORIGINAL RESEARCH

Network Pharmacology Integrated with Transcriptomics Analysis Reveals Ermiao Wan Alleviates Atopic Dermatitis via Suppressing MAPK and Activating the EGFR/AKT Signaling

Ting Xia[1–3], Xiao Liang[4], Chang-Shun Liu[1–3], Yan-Nan Hu[1–3], Zhen-Ye Luo[1–3], Xiao-Mei Tan[1–3]

[1]School of Traditional Chinese Medicine, Southern Medical University, Guangzhou, 510515, People's Republic of China; [2]Guangdong Provincial Key Laboratory of Chinese Medicine Pharmaceutics, Southern Medical University, Guangzhou, 510515, People's Republic of China; [3]Guangdong Provincial Engineering Laboratory of Chinese Medicine Preparation Technology, Guangzhou, 510515, People's Republic of China; [4]School of Pharmaceutical Sciences, Guilin Medical University, Guilin, 541199, People's Republic of China

Correspondence: Xiao-Mei Tan, Tel/Fax + 86-020-61648265, Email tanxm_smu@163.com

Background: Ermiao Wan (EMW) is commonly used to treat atopic dermatitis (AD) in China. However, the pharmacological mechanisms underlying the action of EMW against AD remain unclear.

Purpose: We aimed to determine the mechanisms underlying the effectiveness of EMW in the treatment of AD.

Methods: We evaluated the effect of EMW on AD induced by dinitrochlorobenzene (DNCB) in BALB/C mice. To clarify the key components of EMW in AD treatment, the main components of EMW were identified using HPLC. Serum pharmacochemistry was used to analyze the absorbed ingredients from blood. Based on the phytochemical results, network pharmacology and molecular docking were used to predict the action of EMW. Skin transcriptomic analysis was used to validate the network pharmacology results. RT-qPCR,ELISA, and immunohistochemical were performed to validate the results of skin transcriptomics.

Results: EMW improved the symptoms of AD, with less rashes, less spontaneous scratching, less inflammatory cell infiltration, and fewer allergic reactions. The established HPLC method is simple and reliable. Chlorogenic acid, phellodendrine, magnoflorine, jatrorrhizine, palmatine, berberine, and atractylodin were the key effective ingredients with a high blood concentration. Fifty-seven primary causal targets of EMW against AD were identified. These targets are mainly involved in ErbB signaling pathways including EGFR, AKT1, MAPK8, JUN, MAPK1. Molecular docking showed that EGFR, AKT1, MAPK8, JUN, MAPK1 had good binding force with EMW. In AD mice, EMW regulated the EGFR/AKT signaling through upregulation of Grb2, GAB1, Raf-1, EGFR, and AKT, and downregulation of MAPK1 and JUN, compared to that in the MD group.

Conclusion: EMW could alleviate AD through activating EGFR/AKT signaling and suppressing MAPK. This study provides a theoretical basis for the clinical use of EMW.

Keywords: Ermiao Wan, atopic dermatitis, network pharmacology, serum pharmacochemistry, skin transcriptome, EGFR/AKT signaling

Introduction

Atopic dermatitis (AD) is a common chronic, inflammatory skin disorder characterized by severe pruritus, with a complex pathogenesis and recurrent attacks.[1] It seriously reduces work enthusiasm and life quality, especially in those with moderate to severe AD. Approximately 200 million people worldwide are affected by AD.[2] In addition, with the outbreak of COVID-19, 97.0% of health care workers had skin damage and AD because of enhanced infection-prevention measures.[3,4] Antibiotics are commonly used to relieve AD symptoms. However, there are adverse reactions such as drug resistance, hormone-dependent dermatitis, skin atrophy.[5] Traditional Chinese medicine (TCM) has the advantages of good therapeutic effect, high safety, and less side effects.

Received: 10 August 2022
Accepted: 8 December 2022
Published: 21 December 2022

Ermiao Wan (EMW) is commonly used in the clinical treatment of AD in China. The clinical application of EMW for preventing AD first appeared in the book of Danxi Xinfa, which is from the Ming Dynasty. EMW is used to relieve the symptoms of AD, such as rash and spontaneous scratching.[6] EMW is composed of *Atractylodis Rhizoma* (AR) and *Phellodendri Cortex* (PC) in a 1:1 ratio. PC alleviates the symptoms of specific dermatitis by reducing the phosphorylation of MAPKs, inhibiting the activity of NF-κB, and suppressing M1 polarization of macrophages.[6,7] In addition, the volatile components in AR prevent AD.[8] The alkaloids in EMW have good biological activity,[9,10] which can improve skin pruritus by inhibiting serum Th1/2 cytokines, and suppressing the phosphorylation of JNK, ERK and P38 in the skin.[11] Owing to the multi-component and multi-target characteristics, the mechanisms underlying the therapeutic effects of EMW in AD are unclear. It is difficult to clarify the mechanism of EMW in treating AD using conventional methods.

Network pharmacology is a novel discipline that integrates biology, pharmacology, and informatics.[12] Network pharmacology is suitable for elucidating the synergistic effects of TCM.[13] TCM is comprised of multiple ingredients, which impart consolidated pharmacological effects by modulating different targets and pathways.[14] Network pharmacology can elucidate the interactions between ingredients and their targets; therefore, it is suitable for studying the pharmacological mechanisms of TCM. Network pharmacology is widely used in the prediction of potential active components, targets, and action mechanisms of TCM.[15,16] However, network pharmacology is a theoretical prediction that needs further experimental verification. The combination of animal efficacy validation and transcriptomics analysis can confirm the results of network pharmacology and provide a clear understanding of the mechanism of EMW in treating AD. In this study, we combined method of network pharmacology and transcriptomics to elucidate the mechanism of EMW in the treatment of AD.

Materials and Methods

Materials and Reagents

EMW was purchased from Guangdong Traditional Chinese Medicine Co., Ltd. (Guangzhou, China). Reference standards, including berberine, palmatine, jateorhizine, phellodendrine, magnoflorine, atractylodin, and chlorogenic acid were obtained from the National Institute for the Control of Pharmaceutical and Biological Products (Beijing, China). Acetonitrile was high-performance liquid chromatography (HPLC) grade, purchased from Merck (Darmstadt, Germany). Other reagents were analytical grade. Acetone was purchased from Guangzhou Chemical Reagent Factory (Guangzhou, China). 2,4-Dinitrochlorobenzene (DNCB) was purchased from Shanghai Acmec Biochemical Co., Ltd. (Shanghai, China). Dexamethasone (DEXA) was purchased from Guangzhou Yuanye Biological Co., Ltd. ELISA kit of EGFR, AKT and MAPK were purchased from Jiangsu Meimian industrial Co., Ltd (Yancheng, China).

Animal Study and Experimental Design

Thirty-two male BALB/C mice (5 weeks old with similar body weight 20 ± 2g, animal license No. SCXK (YUE) 2016–0041) were selected from the Experimental Animal Center of Southern Medical University (Guangzhou, China). Mice were housed in a specific pathogen-free (SPF) facility. The animal use protocol and experimental procedures in this experiments were approved by the Institutional Animal Care and Use Committee of the Southern Medical University. Ethical qualification No: L2021097. All the animal procedures were performed in accordance with the Guidelines for Care and Use of Laboratory Animals of the National Institutes of Health.

Mice were randomly divided into four groups (n = 8), normal control group (NC), AD model group (MD), positive control drug dexamethasone group (DEXA), and EMW treatment group (EMW). Except for those in the NC group, AD lesions were induced in all mice using dinitrochlorobenzene (DNCB), as described previously.[17] Briefly, the dorsal hair in a square area of 2×2 cm was shaved. DNCB, a commonly used modeling drug in AD models, was dissolved in an acetone and olive oil mixture (4:1 v/v). After 24 h, the dorsal skin was treated with 1% DNCB solution (200 μL) once a day for 3 consecutive days. Simultaneously, both ears were treated with 0.5% DNCB solution (20 μL) to induce inflammation. In addition, 0.5% DNCB solution (200 μL) was applied to the dorsal skin twice a week for 2 weeks to promote AD lesions. During the experiment, the EMW group and the DEXA group were treated with EMW (1.8 g / kg) and DEXA (1.5 mg / kg) for 14 days (days 5–19, Figure 1A). The NC group and the MD group were administered the

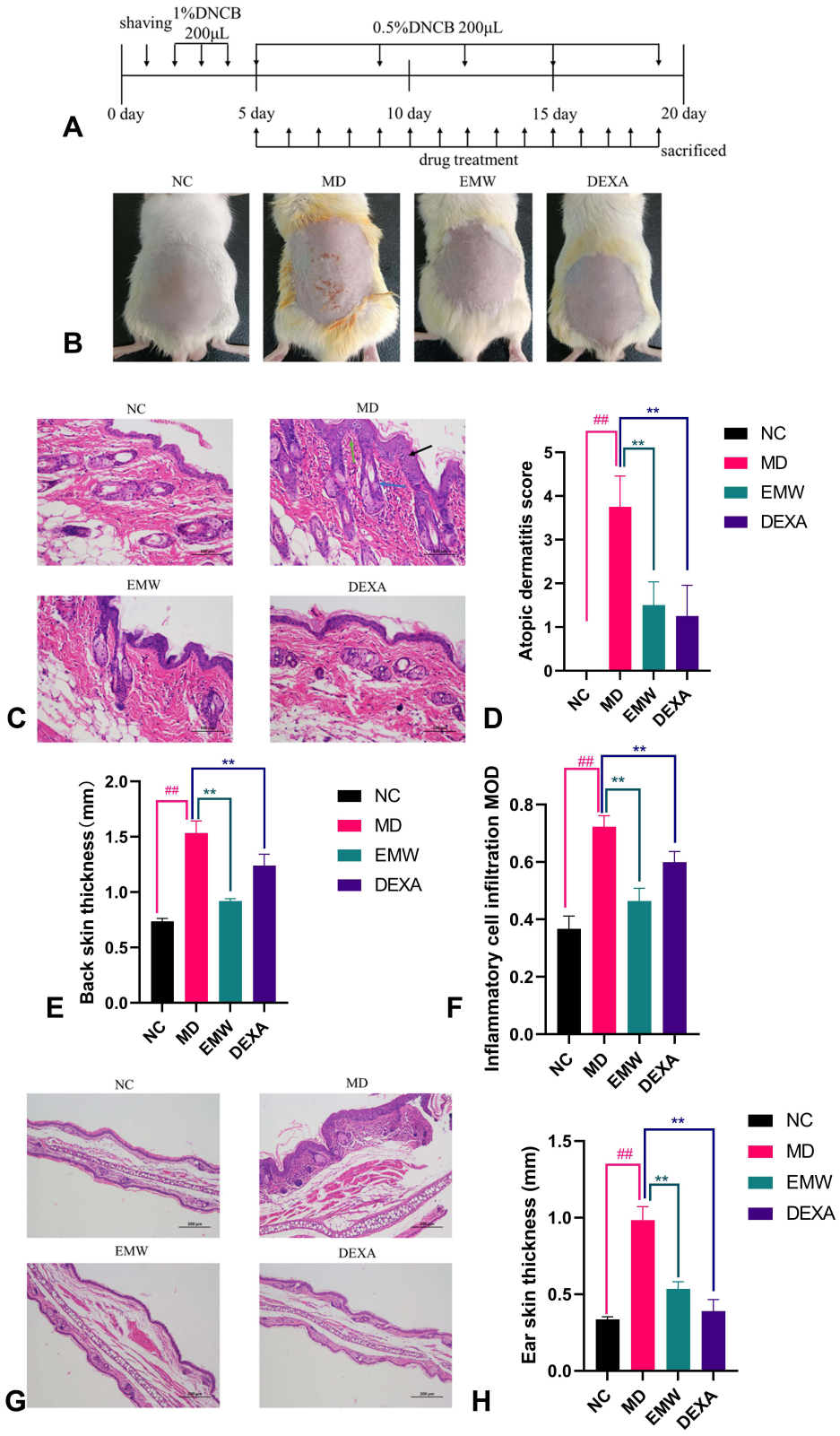

Figure 1 The efficacy of EMW in the treatment of AD. Modeling process of AD mice (**A**); the dorsal skin picture of each group (**B**); the H&E staining of dorsal skin (**C**), the black arrows represent the stratum corneum, the blue arrow represents the spinous layer, the green arrow represents the inflammatory cells; the AD scores of mice in each group (**D**); skin thickness on the back of mice (**E**); inflammatory cell infiltration in mice (**F**); the H&E staining of ear (**G**); the ear skin thickness of mice in each group (**H**). Data are presented as mean ± SD. $^{\#\#}p<0.01$ versus NC group, $^{**}p<0.01$ versus MD group.

https://doi.org/10.2147/DDDT.S384927 DovePress

same dose of normal saline. EMW dose was calculated according to the clinical dosage. The conversion factor for mice and humans is 9.[18] All the animals were sacrificed for collecting the right ears, dorsal skin and serum samples. Samples were collected and stored at −80°C.

Measurement of Skin Score and Ear Thickness

We assessed the severity of erythema, edema, and stretches on the dorsal skin of AD mice, according to Fan's method, before they were sacrificed.[19] A micrometer was used to gauge the thickness of the mice' ears. The mouse atopic dermatitis scoring standard is showed in Table 1.

Hematoxylin and Eosin (H&E) Staining

Dorsal skin and ear tissue samples were fixed in 4% paraformaldehyde (n = 8), and embedded in paraffin blocks. The blocks were cut into 5 μm sections and stained with hematoxylin and eosin (H&E). Histopathological changes were observed using a light microscope.

Quantification of Ingredients from EMW

We weighed 1.0 g EMW and placed it in a 100 mL glass triangle bottle; 50 mL ethanol (v:v = 1:1) added and the mixture was ultrasonicated for 30 min. The extract was filtered using a 200 mesh gauze and centrifuged (1200 × g, 15 min). The supernatant was retained after centrifugation, 5 μL of the supernatant was injected into an HPLC system to determine the components of EMW. Samples were separated on an ZORBAX SB-C18 (4.6 mm× 250 mm, 5 μm) column, with a mobile phase consisting of acetonitrile (A) and 0.1% phosphoric acid (B). The gradient elution was as follows: 0–30 min, 7–18% A; 30–45 min, 18–22.5% A; 45–50 min, 22.5–24% A; 50–55 min, 24–48% A; 55–65 min, 48–51% A; 65–85 min, 51–70% A; 85–90 min, 70–100% A. The wavelengths were as follows: at 0–65 min, 280 nm; at 65–90 min, 330 nm. The flow rate was 1.0 mL/min, and the column temperature was 25 °C.

The method was validated as follows: (1) The reference substances of chlorogenic acid, phellodendrine, magnoflorine, jatrorrhizine, palmatine, berberine, and atractylodin were precisely weighed, then 50% ethanol was added to prepare a series of concentrations of the reference solution. A standard curve was drawn according to the chromatographic conditions with the peak area (Y) and reference substance concentration (X), and a linear regression equation was obtained. (2) The same sample solution was injected continuously six times according to the chromatographic conditions, the chromatographic peak area was recorded, and the precision of the instrument was verified. (3) Six samples of test solution were prepared and used for the chromatographic separation, the content of the components was calculated, and repeatable experimental results were obtained. (4) The content of the components in the same solution was determined within 24 h to obtain experimental stability data. (5) The recovery rate was evaluated by adding a standard and comparing the content of the sample before and after preparation.

Table 1 Criteria of AD Severity

Item	Severity Index	Score
Erythema	None	0
	Mild	1
	Moderate	2
	Severe erythema and mild scar	3
	Severe erythema and scar	4
Oedema	None	0
	Mild	1
	Moderate	2
	Severe	3
Scratching	No	0
	Yes	1

Composition Identification of EMW in Mice Serum

EMW powder (1.0 g) was mixed with 10 mL water and stirred. The serum of mice was collected 2 h after EMW (1.8 g/kg) administration. The serum proteins were precipitated by adding 3 volumes of methanol. The precipitated proteins were collected through centrifugation at 1200 × *g* for 15 min at 4 °C. The supernatant was collected and dried using nitrogen. The serum samples were analyzed using UPLC/ESI-Q-TOF-MS (Agilent 1290, USA). An ACE Excel 3 C18 Column (100 mm × 2.1 mm, 3.0 μm) with a column temperature of 30 °C, and the injection volume was 10 μL. The mobile phase was composed of acetonitrile (A) and 0.1% (v/v) formic acid (B), the flow rate was 0.4 mL/min. The elution gradient was as follows: 0–10 min, 10%-20% B; 10–12.5 min, 25%-40% B; 12.5–20 min, 40%-80% B. The mass spectrometry conditions were as follows, H-ESI ion source detection mode was used, the positive and negative ion scanning range was 50–2000 mppz, the capillary voltage was 3500 V, the dryer flow rate was set at 10 L/min, dryer temperature was 350 °C, ion conversion tube temperature was 320 °C, and atomization pressure was 30 psi. Termo Xcalibur software (version 4.0) was used to collect the data of UPLC/ESI-Q-TOF-MS.

Network Pharmacology Studies

Target Screening

The targets of seven components in EMW were collected on TCMSP database (http://tcmspw.com/tcmsp.php). AD-related targets were obtained by using 'atopic dermatitis' as the keyword in the DisGeNET (https://www.disgenet.org/) database. A Wayne diagram of EMW active ingredient targets and AD targets were drawn using the Venny 2.1 database (https://bioinfogp.cnb.csic.es/tools/venny/). The targets at the intersection were considered as the key targets of EMW in the treatment of AD.

Protein-Protein Interaction (PPI) Network

Key targets were imported into STRING database (https://string-db.org/) to construct PPI model, then use the Cytoscape 3.7.2 software to obtain the PPI network.

Compound-Target Network

The active components and key targets were imported into Cytoscape 3.7.2 to build a compound-target network. Simultaneously, visualization and network topology analyses were carried out to determine the critical degree of EMW targets.

Gene Ontology (GO) and Pathway Enrichment Analysis

To further understand the function of the target and their role in the signal pathway, the top 10 targets were introduced into the DAVID 6.8 database (https://david.ncifcrf.gov/). The list of target gene names was entered the species was defined as 'Homo sapiens'; targets were searched and transformed, and the threshold was set as < 0.5. GO analysis and KEGG pathway analysis were carried out; the results of the top 10 items were visualized.

Molecular Docking

To further verify the binding ability of key targets and compounds, seven compounds in EMW and 10 key points were docked through molecular docking. There were no ligands in the protein structure of the 10th target; therefore, only nine targets were docked. The three-dimensional (3D) structure of the compounds were obtained from ChemDraw, the energy was minimized, and then imported into Sybyl X2.1. The 3D structures of EGFR (ID:5GTY), AKT1 (ID:6HHH), PTGS2 (ID:5F1A), STAT3 (ID:6SMB), MMP9 (ID:2OW0), ICAM1 (ID:3E2M), MAPK8 (ID:3PZE), JUN (ID:2NO3), and MAPK1 (ID:5NHF) were downloaded from the PDB database (https://www.rcsb.org/). Molecular docking was carried out using Surflex-Dock after removing the residues, deoxygenation, and hydrogenation; the other parameters were set at the default values of the system.

Skin Transcriptome Analysis and Verification of Gene Expression

Evaluation of the Skin Transcriptome

Extraction of total RNA, verification of RNA integrity and measurement of RNA concentration was carried out using the RNEasy Mini Kit (Qiagen, USA), RNA Nano 6000 Assay Kit (Agilent, USA) and Qubit® RNA Assay Kit (Thermo-Fisher,

USA), respectively. Sequencing was performed using an Illumina Hiseq platform and 150 bp paired-end reads were produced. Clean data with high quality reads were generated after filtering. Data with an absolute value of fold-change (FC) > 1.0 and p-value < 0.05 (t-test) were identified as differentially expressed genes (DEGs). Enrichment analysis based on GO and KEGG was carried out for functional annotation and biological description of DEGs (http://www.bioinformatics.com.cn).

Verification of Gene Expression Using Real-Time Quantitative Polymerase Chain Reaction (RT-qPCR)

Total RNA was extracted from dorsal skin tissues using TRIzol reagent (Invitrogen™, Thermo Fisher Scientific, America) according to the manufacturer's protocol. The purity and concentration of total RNA were determined using a Nanodrop 4000 spectrophotometer (Thermo Fisher Scientific, MA, America). Reverse transcription and RT-PCR were performed using a Bestar® one-step RT qPCR kit (DBI Bioscience, Ludwigshafen, Germany). All reactions were performed in triplicate and data were analyzed according to the $2^{-\Delta\Delta Ct}$ method. The primer sequences used are summarized in Table 2.

The Expression of EGFR, AKT, and MAPK

Blood samples were collected after the mice were sacrificed; the samples were centrifuged at 1200 × g for 15 min to obtained the serum. All serum samples were analyzed for EGFR, AKT, and MAPK expression using the appropriate mouse ELISA kit, according to the manufacturer's instructions.

Immunohistochemistry (IHC) was carried out to verify the expression of the key proteins in the back skin of mice. Skin sections were used for IHC staining using anti-mouse EGFR, MAPK1 (Servicebio, Wuhan, China), and AKT (Proteintech, Rosemont, IL) antibody (1:100) at 4 °C overnight. All slices were counterstained with hematoxylin at 25 °C for 1 min. Microscopic images were obtained with a light microscope. The results were analyzed by Image J software (National Institutes of Health, USA).

Statistical Analysis

The data are expressed as mean ± standard deviation. Results of the experimental groups were compared by one-way ANOVA using the GraphPad Prism 8.3. Values of $p < 0.05$ or $p < 0.01$ were considered statistically significant or extremely significant, respectively.

Results

EMW Improves DNCB-Induced AD Skin Lesions

AD is induced in the dorsal skin of BALB/C mice following the repeated application of DNCB. The skin condition of mice treated with EMW and DEXA were significantly better than that in the MD group (n = 8) (Figure 1B). After successful modeling, the erythema of the dorsal skin in the MD group was significantly extended compared to that in the NC group. Oral administration of EMW and DEXA reduced the thickness of dorsal skin and ear (Figure 1E and F). Histopathology showed that, mice with DNCB-induced AD showed hyperkeratosis, incomplete keratinization, thickening of the spinous layer, and inflammatory cell infiltration. The symptoms improved after the treatment of EMW and DEXA.

Table 2 Primers Sequences of Related Genes Used for RT-qPCR

Genes	Forward (5′ to 3′)	Reverse (3′ to 5′)
AKT	TTTGGGAAGGTGATTCTGGTG	CAGGACACGGTTCTCAGTAAGC
GAB1	TGGTGGCAGATAGTGAGGAAGA	CTTGGCAGAGTCAAAGAGGGTT
Grb2	GCAGAACTCAATGGGAAAGATGG	CTTCACCACCCACAGGAAATACT
JUN	CACCACTTGCCCCAACAGAT	TTCCTCATGCGCTTCCTCTCT
MAPK	CCAAGGGTTATACCAAGTCCATT	TCCAAGAATACCCAGGATGTGA
Raf-1	CCGAATAAGCAAAGGACTGTGG	AGCGTGCTTTCTTACCTTTGTG
β-action	GTGACGTTGACATCCGTAAAGA	GTAACAGTCCGCCTAGAAGCAC

These results indicate that EMW can effectively treat epidermal damage and the production of inflammatory factors in AD (Figure 1C and D).

HPLC and UPLC/ESI-Q-TOF-MS Analysis of Major Ingredients in EMW

The main components of TCM should be present at a high concentration and have high biological activity for them to be effective application. The main components of EMW were identified through HPLC fingerprints. Based on the content and bioactivity, seven components in EMW were considered as the main biological components (Figure 2A). Six batches of EMW samples were analyzed individually; six high similarity maps were obtained. This method offers repeatability and stability (Figure 2B). The chemical structures of the main components in EMW were illustrated Figure 2C. The concentrations of the major components in EMW were as follows: chlorogenic acid, 1.52 ± 0.48 mg/mL; phellodendrine, 7.62 ± 0.81 mg/mL; magnoflorine, 0.62 ± 0.34 mg/mL; jateorhizine, 0.42 ± 0.26 mg/mL; palmatine, 0.02 ± 0.004 mg/mL; berberine, 49.68 ± 1.38 mg/mL; and atractydin, 38.43 ± 0.92 mg/mL. These seven compounds represented the major bioactive components of EMW, therefore, they were used for subsequent network pharmacology analysis.

Following the oral administration of EMW, the seven components that were at a high concentration and exhibited good biological activity were identified in the serum of mice through UPLC/ESI-Q-TOF-MS analysis. The main ingredients are chlorogenic acid, phellodendrine, magnolamine, jatrorrhizine, palmatine, berberine, and atractylodin (Figure 3 and Table 3).

Network Pharmacology Results

The chemical components and AD-related targets were screened, as described previously.[20] There were 788 and 295 targets related to AD and EMW, respectively. Among them, 57 targets were identified as potential targets of EMW in treating AD (Figure 4A). PPI network indicated the interaction between targets; fifty-seven target nodes were connected by 318 edges, with an average of 11.2 node degree and 0.548 local clustering coefficient. The PPI enrichment *P*-value was < 1.0 e^{-16} (Figure 4B). The top 10 hub genes included EGFR, AKT1, PTGS2, STAT3, MMP9, ICAM1, MAPK8, JUN, MAPK1, and VCAM1. The darker the color of the node, the larger the size, which indicates that the protein may be more crucial in the treatment of AD (Figure 4B and C) shows the compounds and targets network.

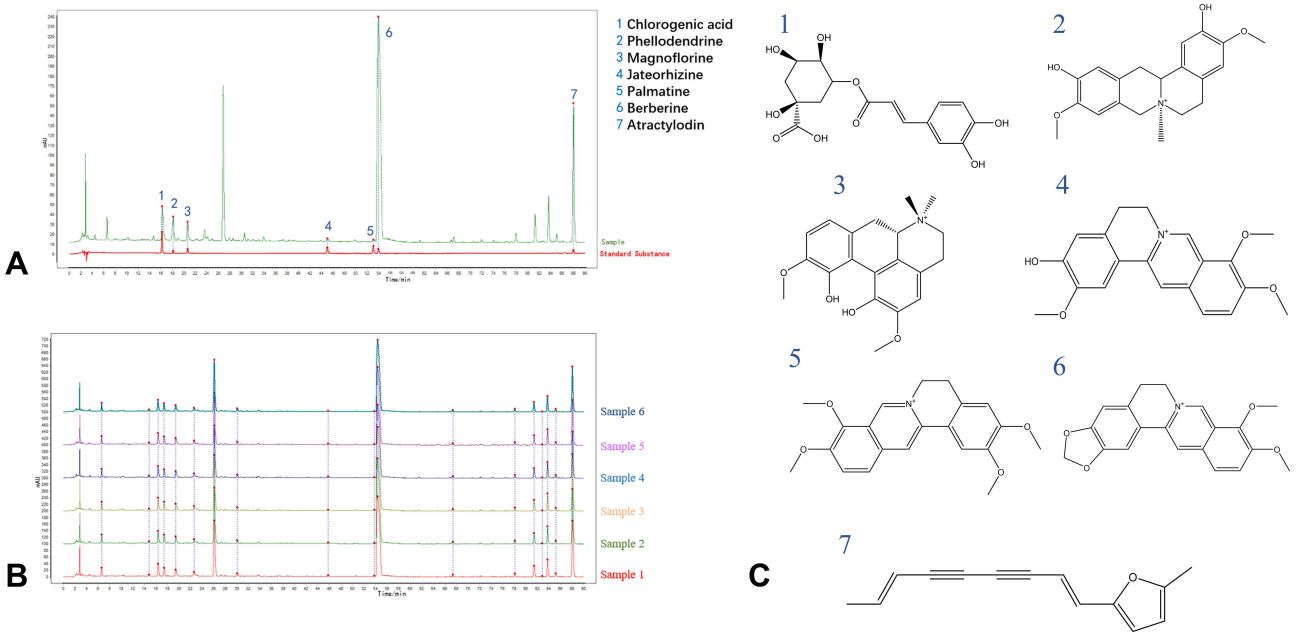

Figure 2 Representative HPLC-based chemoprofiles of EMW samples. Ingredient identify of the EMW by HPLC fingerprint (**A**) and repeatability analysis(**B**). The structures of analytes which label as following: 1. chlorogenic acid, 2. phellodendrine, 3. magnoflorine, 4. jateorhizine, 5. palmatine, 6. berberine, and 7, atractylodin (**C**).

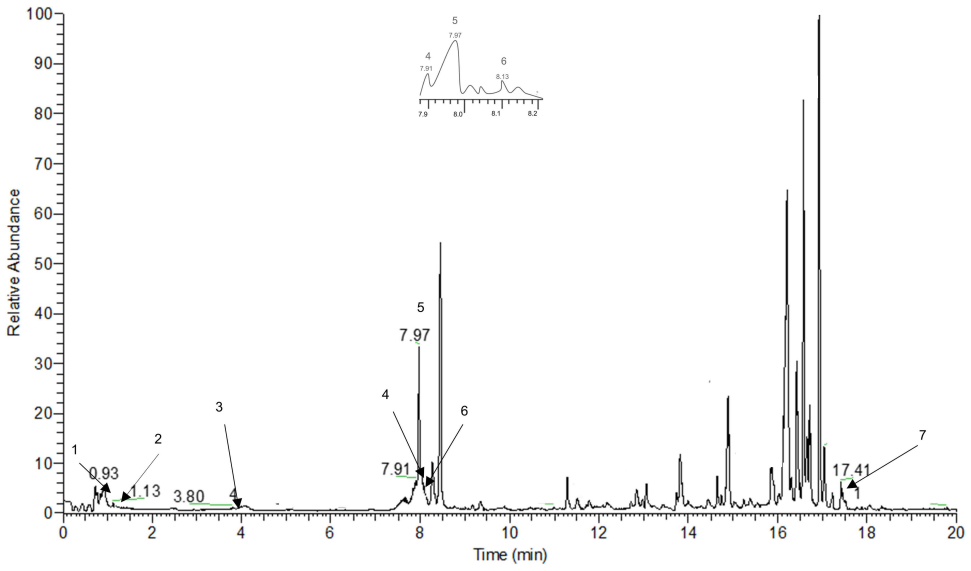

Figure 3 Total ion current chromatogram of UPLC/ESI-Q-TOF-MS of EMW in mice serum.

GO analysis results revealed 76 terms of biological processes, and the core terms of EMW targets with AD were mainly involved in the negative regulation of apoptosis process, positive regulation of vasoconstriction, nitric oxide biosynthetic process, smooth muscle cell proliferation, cellular response to mechanical stimulus, aging, response to drug, positive regulation of transcription from RNA polymerase II promoter, signal transduction, and regulation of sequence-specific DNA binding transcription factor activity (Figure 5A and B). The 71 enriched KEGG pathways ($p < 0.05$) included the TNF signaling pathway, pathways in cancer, hepatitis B, pancreatic cancer, ErbB and estrogen signaling pathway, Epstein-Barr virus infection, choline metabolism in cancer, hepatitis C, and FOXO signaling pathways (Figure 5C and D).

Based on the compound-target network and pathway enrichment analysis results, we created a compound-target-pathway network consisting of the top 10 KEGG pathways (Figure 5E). The network showed that EMW and AD shared 10 KEGG pathways, indicating their common anti-AD targets. Moreover, ErbB signaling pathway associated with key targets, was attributed with the EMW effects on AD. Network pharmacology revealed the importance of EGFR, AKT1, MAPK8, MAPK1, and JUN. Therefore, EMW could alleviate the anaphylactic reaction and the immunologic and exert synergistic effects against AD.[21]

Molecular Docking

The components with high concentration were docked with the key targets. The molecular docking principle suggests that a docking fraction greater than 4.25 indicates that the molecule has a strong binding ability with the target.[22] Among

Table 3 UPLC-Q-TOF-MS Data of Main Active Components in Mice After Oral Administration of EMW

No	t_R/min	Identification	Formula	Measured Mass (m/z)	|Error|/ppm	Source
1	0.93	Phellodendrine	$C_{20}H_{24}NO_4^+$	342.17047	0.08772	PC
2	1.13	Ferulic Acid	$C_{10}H_{10}O_4$	194.05788	0.10309	PC, AL
3	3.80	Magnoflorine	$C_{20}H_{24}NO_4^+$	342.17071	0.614035	PC
4	7.91	Jateorhizine	$C_{20}H_{20}NO_4^+$	338.13841	2.33728	PC
5	7.97	Berberine	$C_{20}H_{18}NO_4^+$	336.12376	0.47619	PC
6	8.13	Palmatine	$C_{21}H_{22}NO_4^+$	352.15486	0.11364	PC
7	17.41	Atractylodin	$C_{13}H_{10}O$	182.07316	0.21978	AL

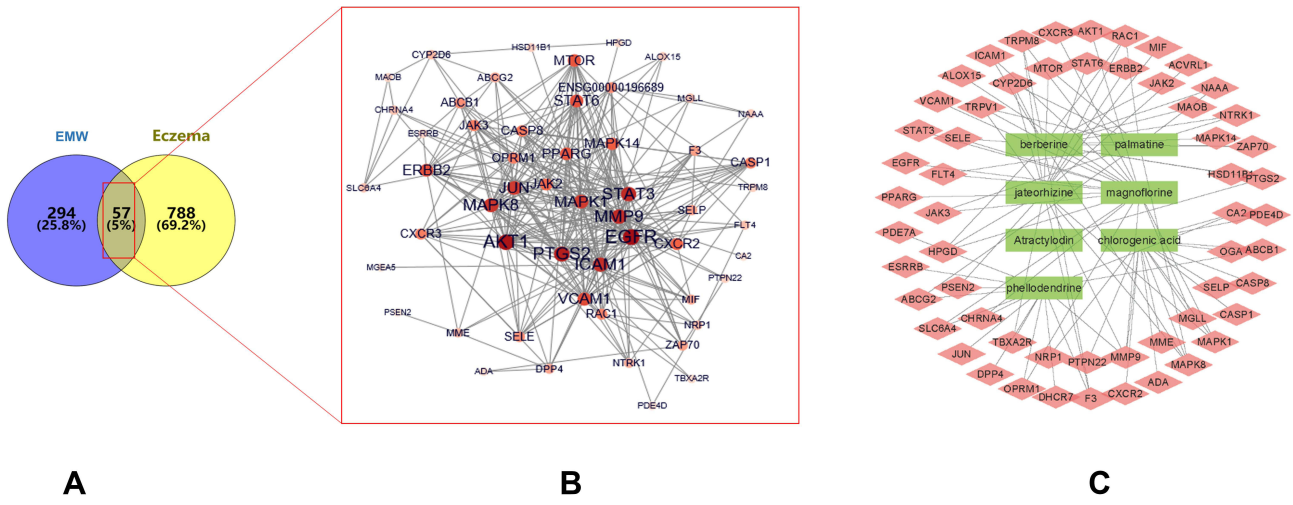

Figure 4 Key targets and compounds. Targets attribution among the EMW and AD (**A**). Protein-protein interaction network of crossover targets. Node, target protein (**B**). Ingredients -target-pathway network. Labels: Green squares, ingredients; Pink diamonds, protein targets (**C**).

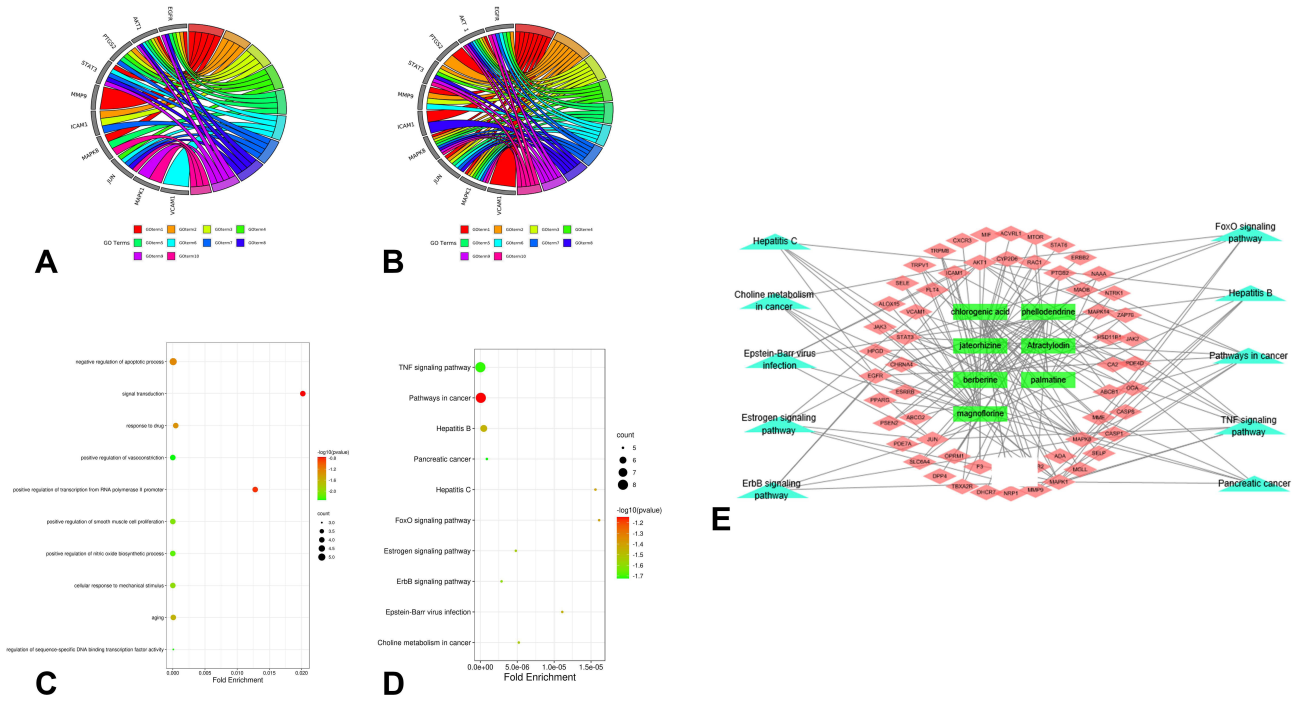

Figure 5 Potential mechanisms of EMW treat AD. (**A**) Core biotargets of EMW against AD were related to the top 10 enriched GO terms in circro diagrams. (**B**) Biological processes were presented by bubble diagrams generated through count algorithms and – log (*P*-value) calculation. (**C**) Core biotargets of EMW against AD were linked to the top 10 enriched KEGG terms in circro diagrams. (**D**) Molecular pathways (from KEGG analysis) were presented by bubble diagrams based on counting algorithms and – log (*P*-value). (**E**) Compound-target-pathway network of EMW and AD. Labels: green squares, ingredients, pink diamonds, protein targets, cyan triangle, pathways.

the key targets, EGFR, AKT1, and PTGS2 bind well with all components. Palmatine, phellodendrine, chlorogenic acid, and jatrorrhizine bind well with all docking targets (Figure 6). While atractylodin exhibited a binding efficiency of 3 (33.33%) with the docking targets, ICAM1 exhibited a binding efficiency of 2 (28.57%) with the EMW components. Therefore, not every component has a good binding efficiency for every target; however, the interaction between the components and each targets corresponds with the multi-component and multi-target characteristic of TCM.[23]

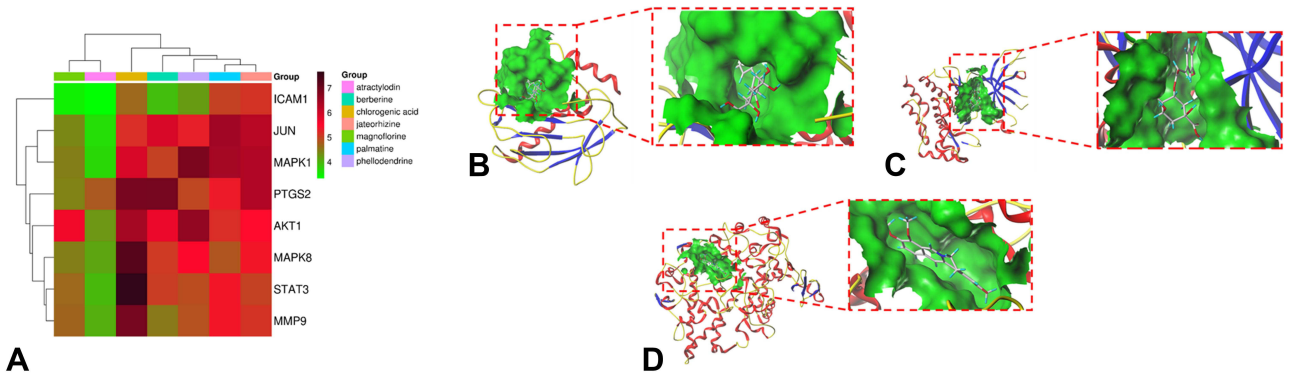

Figure 6 Molecular docking result. (**A**) Heatmap of molecular docking result. (**B**) The three-dimensional mode of chlorogenic acid in the active site of MMP9. (**C**) The three-dimensional mode of chlorogenic acid in the active site of STAT3. (**D**) The three-dimensional mode of berberine in the active site of PTGS2.

Transcriptome Analysis Revealed the Signal Pathway of EMW in Treating AD

Visualization of DEGs

A total of 530 DEGs were identified in the MD group compared with the NC group, of which 461 were up-regulated and 69 down-regulated (Figure 7A). The heatmap of 530 DEGs was shown in Figure 7B. Compared with the MD group, a total of 441 DEGs were identified in the EMW group, 282 of which were up-regulated and 159 were down-regulated (Figure 7E). The heatmap of the DEGs between the EMW and MD groups is shown in Figure 7F. The Venn diagram shows that EMW treatment could reverse the levels of 36 DEGs induced by AD; 8 genes exhibited restored down-regulation and 28 genes showed restored up-regulation (Figure 7I and J). Therefore, these 36 DEGs were considered as the therapeutic targets of AD. The heatmap of the DEGs that were reversed by AD treatment are shown in Figure 7K.

GO and KEGG Analysis of DEGs

Transcriptomics-based enrichment analysis was further conducted to reveal the potential mechanisms involved in EMW. GO enrichment of DEGs in MD vs NC and EMW vs MD were visualized (Figure 7C and G). The scatterplot for the top 10 enriched KEGG pathways of DEGs in MD vs NC and EMW vs MD are shown in Figure 7D, H and L displays the scatterplot of the DEGs that were reversed by EMW. The KEGG pathway analysis found that the therapeutic targets of AD were mainly enriched in the PI3K-AKT, AMPK, and ErbB signaling pathways.

RT-qPCR

Based on the results of network pharmacology, the EGFR/AKT signaling pathway was considered as the key pathway activated by EMW in the treatment of AD. Gene expression evaluation through quantitative reverse transcription RT-qPCR showed that, the levels of Grb2, GAB1, Raf-1, and AKT in the MD group were significantly lower, while the expression of JUN and MAPK1 were significantly higher compared to that in the NC group. Following the treatment with EMW, the expression of Grb2, GAB1, Raf-1 and AKT was increased significantly in the EMW group, and the levels of JUN and MAPK1 were inhabited (Figure 8).

The Expression of EGFR, AKT and MAPK in AD Mice

To further verify the results of network pharmacology and skin transcriptome, we measured the expression of EGFR, AKT, and MAPK in the serum of mice. The ELISA results showed that the levels of EGFR and AKT in the serum of the MD group were significantly suppressed, while the expression of MAPK was increased, compared to that in the NC group. Following the oral administration of EMW, the levels of EGFR and AKT were increased, while that of MAPK was decreased significantly (Figure 9A–C).

The expression of EGFR, MAPK1, and AKT in the back skin of mice was verified through IHC. The expression of MAPK1 was higher, while the levels of EGFR and AKT were significantly lower in the back skin of mice compared to that in the NC group. After oral administration of EMW, the expression of MAPK1 was down-regulated (Figure 9E and H), and

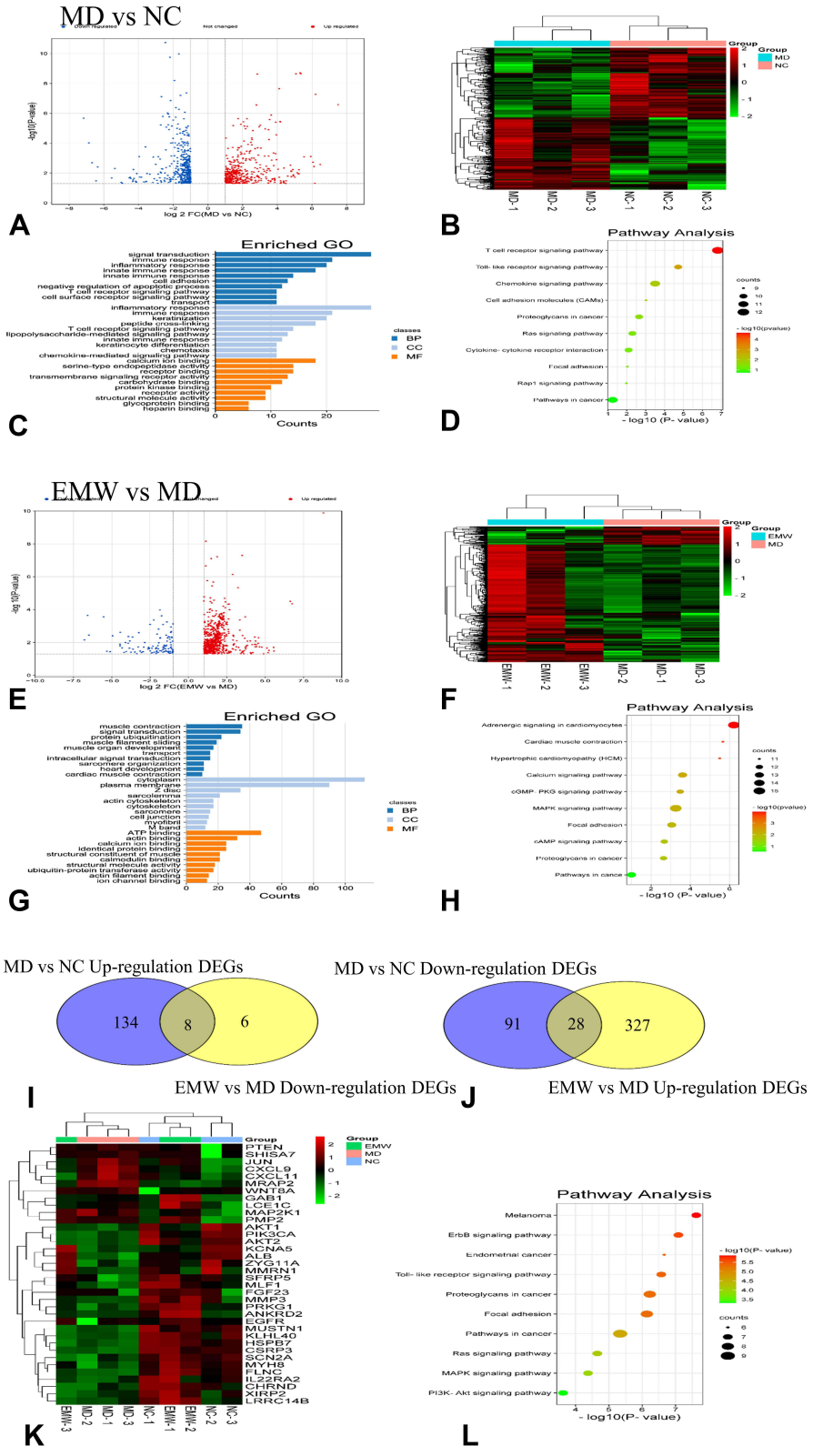

Figure 7 Skin transcriptomics analysis of effects of EMW of AD treatment. The DEGs are represented as a volcano figure (**A**), heatmap (**B**), GO enrichment (**C**) and scatterplot (**D**) comparing the MD and NC groups. The DEGs represented as a volcano (**E**), heatmap (**F**), GO enrichment (**G**) and scatterplot (**H**) comparing EMW and MD groups. Venn diagrams (**I** and **J**), heatmap (**K**) and scatterplot (**L**) revealing DEGs regulated by EMW treatment.

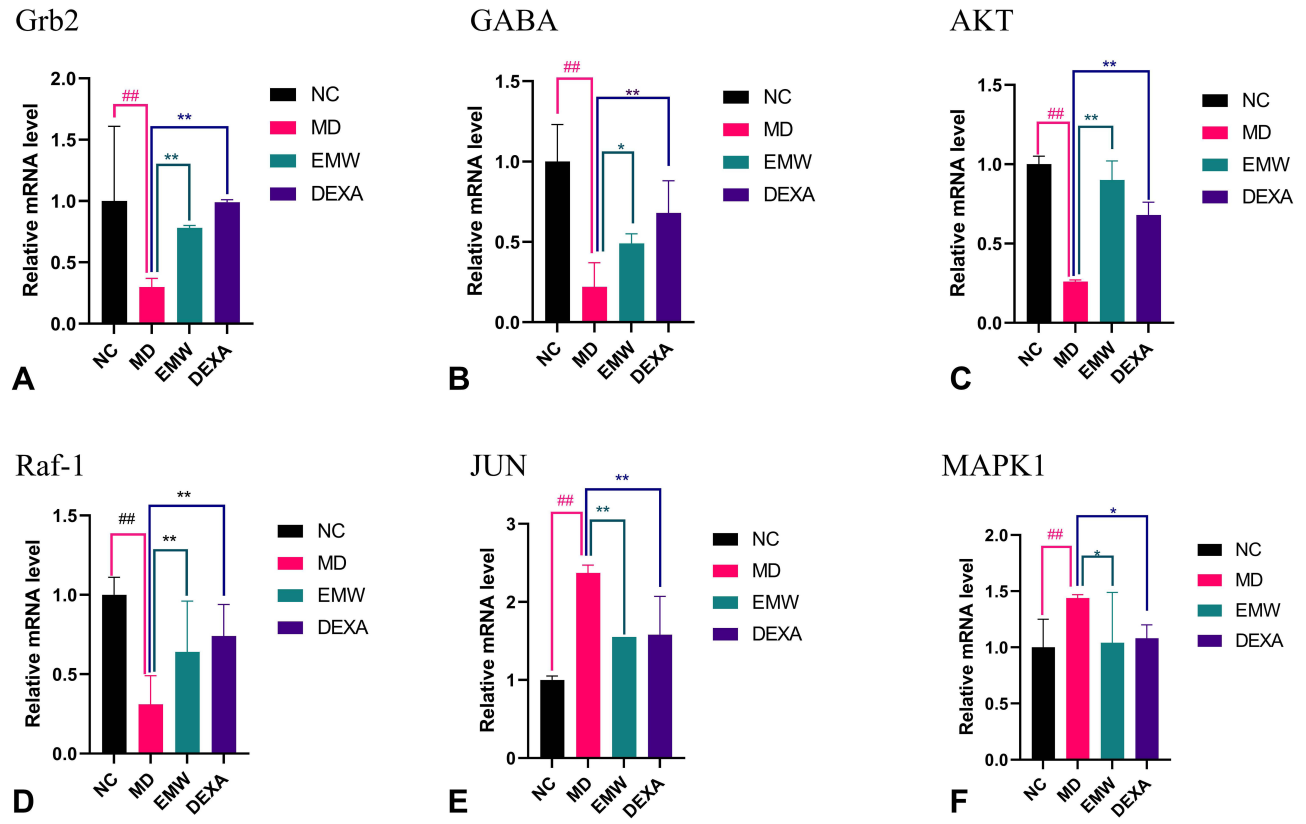

Figure 8 The mRNA level results of all groups in dorsal skin of mice. The relative mRNA level of Grb2 (**A**), GAB1 (**B**), Raf-1 (**C**), AKT (**D**), JUN (**E**) and MAPK1 (**F**). Data are presented as mean ± SD. $^{\#\#}p<0.01$ versus NC group, $^{*}p<0.01$ versus MD group, $^{**}p<0.01$ versus MD group.

the levels of EGFR and AKT were up-regulated significantly (Figure 9D, F, G, and I). The IHC results further confirmed the results of network pharmacology and RT-qPCR (Figure 9A–C).

Discussion

Atopic dermatitis (AD) is one of the most common chronic inflammatory skin diseases, characterized by pruritus, skin damage, and inflammation.[24] AD is characterized by sensitive and dry skin, localized or disseminated eczema, usually accompanied by severe itching. Among the skin diseases, AD has the highest incidence of about 20% of children and 2% of adults worldwide. The pathogenesis of AD is complicated. Heredity, environment, skin barrier destruction and immune dysfunction are currently recognized causes of AD. So far, AD is deemed to be only a skin disease, and local anti-inflammatory drugs are the first-line method in clinical. The drugs that against AD included various topical corticosteroids (TCSs), tacrolimus and pyrrolimus, as well as antihistamines and immunosuppressants.[25] However, these are under a variety of adverse reactions when utilised for a long time or in large doses. Soaring medical costs reduced their clinical value although many effective biological agents have been used for treatment in AD in recent years. Decline in patients' quality of life and certain mortality make AD a global health problem. Therefore, it is necessary to develop AD drugs with less side effects and low prices in clinical.

In this study, we explored the effects of EMW in treating AD through network pharmacology, transcriptomics and experimental verification. Our findings demonstrated that EMW can improve the clinical symptoms of AD by reducing skin score, ear and back skin thickness, and protecting against epidermal skin damage in mice. The clinical therapeutic effect of EMW was similar to that of DEXA. The DEXA group had side effects such as increased food intake and gastrointestinal bleeding. However, the EMW group showed no side effects. Therefore, EMW has lesser side effects but similar AD curative effects as that of DEXA. To the best of our knowledge, this is the first study to determine the mechanism of EMW in treating AD. EMW upregulated Grb2, GAB1, Raf-1, EGFR, and AKT and inhibited MAPK1 and

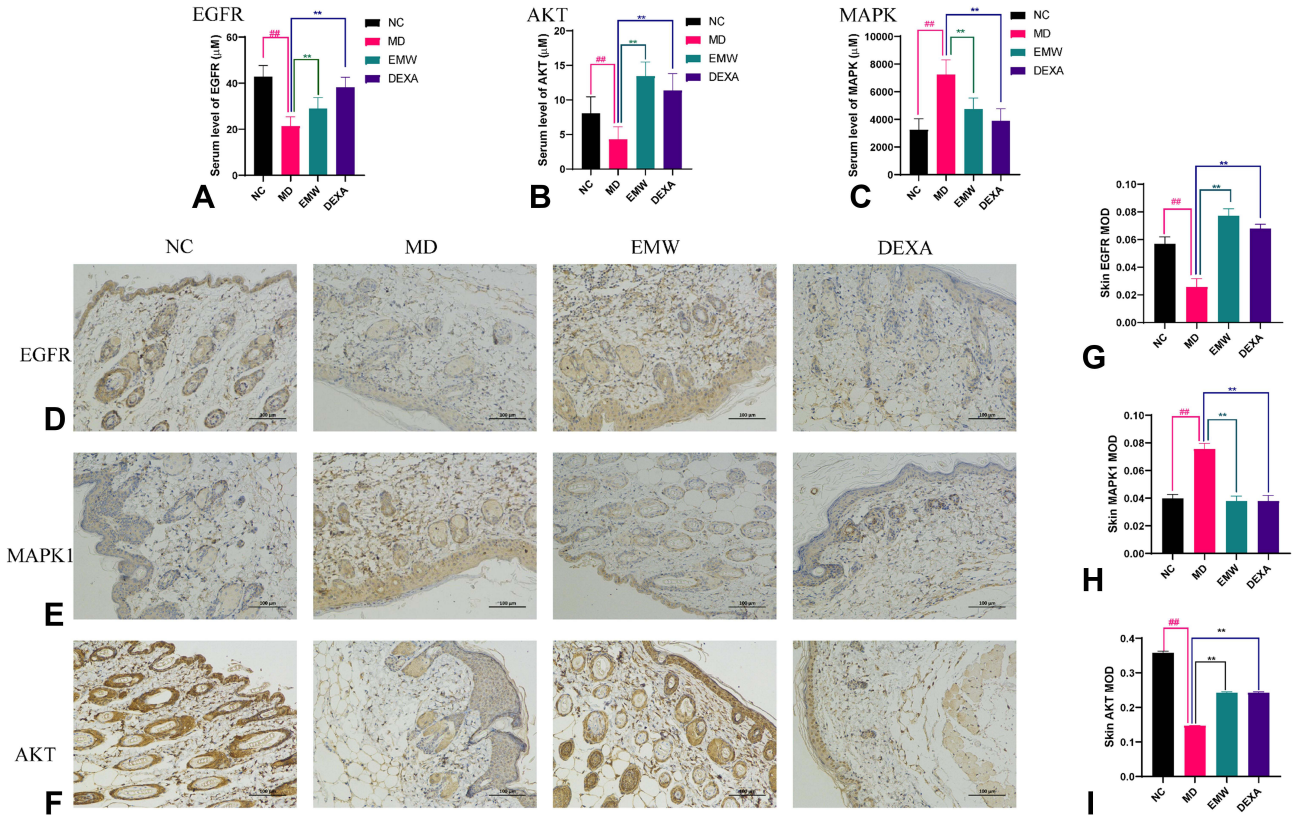

Figure 9 The expression of EGFR (**A**), AKT (**B**) and MAPK (**C**) in each group of serum. Immunohistochemistry results of EGFR (**D, G**), MAPK1 (**E** and **H**) and AKT (**F** and **I**) in each group of skin. Data are presented as mean ± SD. $^{\#\#}p<0.01$ versus NC group, $^{**}p<0.01$ versus MD group.

JUN in AD mice. This could be related to the effects of chlorogenic acid, phellodendrine, magnolamine, jatrorrhizine, palmatine, berberine, and atractylodin.

Effective ingredients are hypothesized to be present at high concentration in the blood. HPLC and UPLC/ESI-Q-TOF-MS were used to identify the key components of EMW that alleviates AD. Chlorogenic acid, phellodendrine, magnolamine, jatrorrhizine, palmatine, berberine, and atractylodin were the main components of EMW. Among them, berberine has the highest blood concentration. Berberine is widely used in the treatment of AD in China,[26] it regulates skin oxidative stress and improves skin condition through antioxidation and AMPK activation.[27] Chlorogenic acid reduces the levels of pro-inflammatory cytokines such as TNF-α and IL-2, and elevates the expression levels of anti-inflammatory cytokines such as IL-4 and IL-13.[28] In addition, chlorogenic acid reduces inflammation through the miR-22-3p /SIRT1 axis.[29] Magnolamine attenuates inflammation by inhibiting MAPK and NF- κ B signaling.[30] This anti-inflammatory effect is related to the inhibition of excessive production of NO.[31] Palmatine inhibits NF- κ B signaling pathway and has potent anti-inflammatory effect.[32,33] Atractylodin regulates the production of inflammatory factors by inhibiting MAPK and NF- κ B signaling pathways.[34] AD is an inflammatory skin disease. The anti-inflammatory effect of the drugs is the key in the treatment process. Therefore, it further substantiates that the effective components of EMW defined in this study play an important role in the treatment of AD.

The main components were used to predict AD-related targets through network pharmacology. Pathway analysis showed that EMW alleviates AD mainly through the ErbB signaling pathway. The ErbB receptor, from the tyrosine kinase family including ErbB1/EGFR/HER1 cell surface receptors, are related to the occurrence of inflammation.[35,36] EGFR and MAPK are the key targets of ErbB signaling pathway. Molecular docking results showed that the effective components of EMW had good binding with EGFR. Chlorogenic acid had the highest docking score (7.2720) with MAPK8. Phellodendrine had the best binding with MAPK1 with a score of 6.8556. The results further indicated that EMW improves AD symptoms by regulating the ErbB signaling pathway.

The pathological features of AD are skin damage and inflammation. Therefore, reducing inflammation and improving skin symptoms are the key strategies in managing AD. Based on the pathway enrichment and skin transcriptome results, we speculate that the EGFR/AKT signaling pathway could be the key mechanism of EMW in treating AD. To further validate our hypothesis, RT-qPCR, ELISA and IHC analyses were conducted. Compared with that in the MD group, EMW upregulated of EGFR, Grb2, GAB1, Raf-1, and AKT in mice skin, and inhibited MAPK and JUN. EGFR, AKT1 and JUN have anti-inflammatory pharmacological effects; certain nonsteroidal anti-inflammatory drugs modulate cellular glycosaminoglycan synthesis by regulating the EGFR and PI3K signaling pathways.[37,38] EGFR is the epidermal growth factor receptor, which plays an essential signaling role in skin biology and inflammatory/immune responses in the skin.[39] Inhibiting EGFR in the cuticle cells enhances inflammation in the skin.[40] In the transcriptional and immunohistochemical analysis of specific dermatitis, the expression of EGFR and ErbB2 is down-regulated.[41] In this study, the expression of EGFR in the EMW-treated group was higher than that in the MD group. In addition, berberine had the highest binding score with EGFR, which further proves that EGFR is the key target of EMW in AD treatment. AD is characterized by AKT1 dysfunction and keratinization; the deletion of AKT1 could be the mechanism underlying specific dermatitis such as AD.[42] Down-regulation of ICAM-1 expression through the activation of AKT is one of the mechanisms underlying AD treatment.[43] Interestingly, RT-qPCR and ELISA both indicate that EMW increase AKT in the MD group. In addition, molecular docking showed that palmatine, chlorogenic acid and jateorhizine could regulate ICAM. Therefore, we conclude that increasing AKT could alleviate AD.

The allergic inflammatory response is associated mainly with the activation of the MAPKs, which include the extracellular signal–regulated kinase, c-Jun N-terminal kinase, and p38MAPK. MAPKs are involved in the activation of the transcription of inflammatory and allergy-related mediators. Inhibition of MAPK signaling pathway and reduction of inflammatory factors are beneficial in treating AD.[44] AD drugs significantly reduce the level of p38MAPK and the activation of NF- κB signaling pathway.[45] The use of MAPK inhibitors could be a therapeutic strategy for allergic skin inflammation.[46] Inhibiting the MAPK signaling pathway and modulating the internal signaling pathway associated with atopic inflammation can significantly reduce the symptoms of AD.[47] Regulation of the MAPK pathways is considered vital for AD prevention.[48] Compared to that in the MD group, MAPK was inhibited in both the DEXA and the EMW groups. MAPK1 and MAPK8 can bind with chlorogenic acid, phellodendrine, magnolamine, jatrorrhizine, palmatine and berberine. These further substantiate and support the results from this study.

Therefore, activating the EGFR/AKT signaling pathway and suppressing MAPK could alleviate inflammation and improve the skin barrier, which could be the mechanism underlying AD treatment (Figure 10).

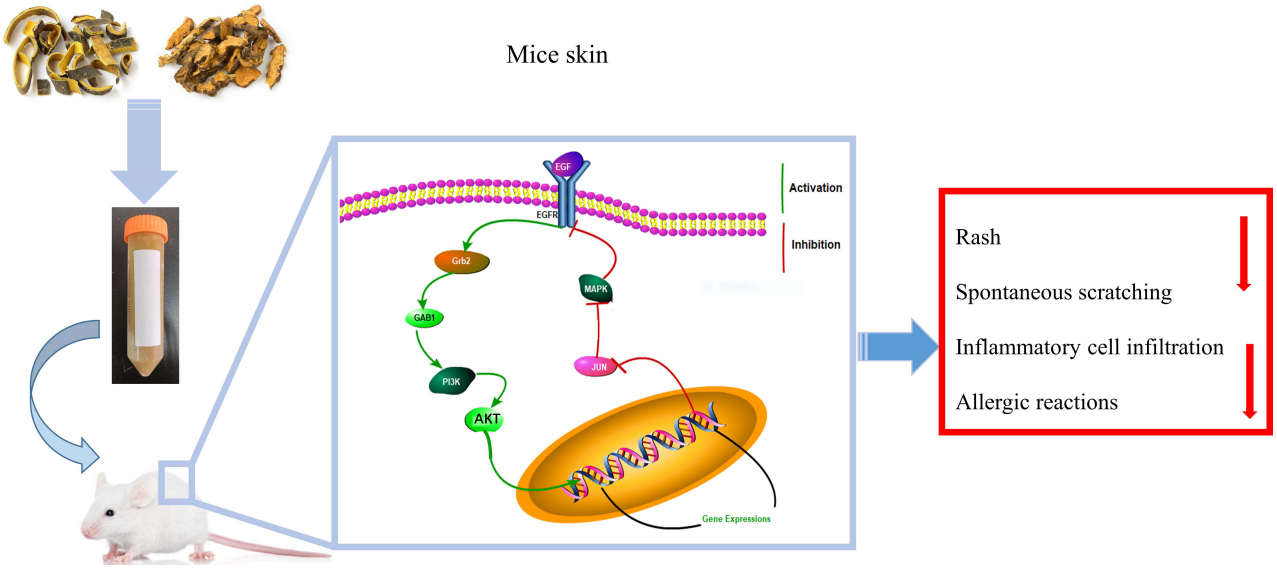

Figure 10 Underlying mechanism of EMW treats AD.

Conclusions

Treatment with EMW decreased AD skin score, reduced ear and back skin thickness in mice, improved skin epidermal damage, and reduced the production of inflammatory factors. Concentration determination and serum pharmacochemistry analysis showed that the key effective components of EMW against AD were berberine, palmatine, jateorhizine, phellodendrine, magnoflorine, atractylodin, and chlorogenic acid. Network pharmacology and skin transcriptome analysis further proved that EMW alleviates AD by activating the EGFR/AKT signaling pathway and inhibiting the expression of MAPK. This is the first study to elucidate the mechanism underlying the therapeutic effects of EMW in AD. This study provides a theoretical basis for the clinical use of EMW.

Highlights

1. EMW improves the clinical symptoms in mice with AD.
2. Berberine, palmatine, jateorhizine, phellodendrine, magnoflorine, atractylodin, and chlorogenic acid are the main pharmacologically active ingredients of EMW in alleviating AD.
3. EMW alleviates AD by inhibiting MAPK and activating the EGFR/AKT signaling pathways.

Abbreviation

AKT1, RAC-alpha serine; AD, atopic dermatitis; AR, *Atractylodis Rhizoma*; DEGs, differentially expressed genes; DEXA, Dexamethasone; DNCB, Dinitrochlorobenzene; EGFR, epidermal growth factor receptor; EMW, Ermiao Wan; GO, Gene Ontology; H&E, Hematoxylin and Eosin Staining; HPLC, high performance liquid chromatography; JUN, transcription factor AP-1; MAPK1, mitogen-activated protein kinase 1; MAPK8, mitogen-activated protein kinase 8; MD, atopic dermatitis group; MMP9, matrix metalloproteinase-9; NC, normal control group; PBS, phosphate buffer saline; PC, *Phellodendri Cortex*; PPI, protein-protein interaction; RT-qPCR, real-time quantitative polymerase chain reaction; TCM, Traditional Chinese medicine; UPLC-Q/TOF-MS, ultra-performance liquid chromatography-quadrupole /time-of-flight mass spectrometry.

Data Sharing Statement

The data and materials in this study are available from the corresponding author upon request.

Ethics Approval and Consent to Participate

The animal use protocol and experimental procedures in this experiments were approved by the Institutional Animal Care and Use Committee of the Southern Medical University. All the animal procedures were performed in accordance with the Guidelines for Care and Use of Laboratory Animals of the National Institutes of Health.

Author Contributions

All authors made a significant contribution to the work reported, whether that is in the conception, study design, execution, acquisition of data, analysis and interpretation, or in all these areas; took part in drafting, revising or critically reviewing the article; gave final approval of the version to be published; have agreed on the journal to which the article has been submitted; and agree to be accountable for all aspects of the work.

Funding

This work is supported by grants from the National Key R&D Program of China (2018YFC1704500; 2018YFC1704503).

Disclosure

The authors declare that they have no conflict of interest.

References

1. Sawangjit R, Dilokthornsakul P, Lloyd-Lavery A, et al. Systemic treatments for eczema: a network meta-analysis. *Cochrane Database Syst Rev*. 2020;9:D13206. doi:10.1002/14651858
2. Flohr C, Mann J. New insights into the epidemiology of childhood atopic dermatitis. *Allergy*. 2014;69(1):3–16. doi:10.1111/all.12270
3. Singh M, Pawar M, Bothra A, et al. Overzealous hand hygiene during the COVID 19 pandemic causing an increased incidence of hand eczema among general population. *J Am Acad Dermatol*. 2020;83(1):e37–e41. doi:10.1016/j.jaad.2020.04.047
4. Lan J, Song Z, Miao X, et al. Skin damage among health care workers managing coronavirus disease-2019. *J Am Acad Dermatol*. 2020;82(5):1215–1216. doi:10.1016/j.jaad.2020.03.014
5. Chong M, Fonacier L. Treatment of eczema: corticosteroids and beyond. *Clin Rev Allergy Immunol*. 2016;51(3):249–262. doi:10.1007/s12016-015-8486-7
6. Chen Y, Xian Y, Lai Z, et al. Anti-inflammatory and anti-allergic effects and underlying mechanisms of Huang-Lian-Jie-Du extract: implication for atopic dermatitis treatment. *J Ethnopharmacol*. 2016;185:41–52. doi:10.1016/j.jep.2016.03.028
7. Zhang M, Cheng J, Hu J, et al. Green Phellodendri Chinensis Cortex-based carbon dots for ameliorating imiquimod-induced psoriasis-like inflammation in mice. *J Nanobiotechnology*. 2021;19(1):105. doi:10.1186/s12951-021-00847-y
8. Fu X, Zhou J, Tang W, et al. Study on the compatibility effect and active constituents of atractylodis rhizoma in ermiao wan against acute gouty arthritis. *J Ethnopharmacol*. 2021;279:114353. doi:10.1016/j.jep.2021.114353
9. Zhang H, Zhang S, Wang W, et al. Characterizing metabolites and potential metabolic pathways changes to understanding the mechanism of medicinal plant Phellodendri Amurensis cortex against doxorubicin-induced nephritis rats using UPLC-Q/TOF-MS metabolomics. *J Pharm Biomed Anal*. 2020;188:113336. doi:10.1016/j.jpba.2020.113336
10. Huang J, Guo W, Cheung F, Tan HY, Wang N, Feng Y. Integrating network pharmacology and experimental models to investigate the efficacy of coptidis and scutellaria containing huanglian jiedu decoction on hepatocellular carcinoma. *Am J Chin Med*. 2020;48(1):161–182. doi:10.1142/S0192415X20500093
11. Zhang R, Zhang H, Shao S, et al. Compound traditional Chinese medicine dermatitis ointment ameliorates inflammatory responses and dysregulation of itch-related molecules in atopic dermatitis. *Chin Med*. 2022;17(1):3. doi:10.1186/s13020-021-00555-7
12. Li R, Wu K, Li Y, et al. Integrative pharmacological mechanism of vitamin C combined with glycyrrhizic acid against COVID-19: findings of bioinformatics analyses. *Brief Bioinform*. 2021;22(2):1161–1174. doi:10.1093/bib/bbaa141
13. Liu CS, Xia T, Luo ZY, et al. Network pharmacology and pharmacokinetics integrated strategy to investigate the pharmacological mechanism of Xianglian pill on ulcerative colitis. *Phytomedicine*. 2021;82:153458. doi:10.1016/j.phymed.2020.153458
14. Li S, Zhang B. Traditional Chinese medicine network pharmacology: theory, methodology and application. *Chin J Nat Med*. 2013;11(2):110–120. doi:10.1016/S1875-5364(13)60037-0
15. Wang Y, Sun YW, Wang YM, et al. Virtual screening of active compounds from Artemisia argyi and potential targets against gastric ulcer based on Network pharmacology. *Bioorg Chem*. 2019;88:102924. doi:10.1016/j.bioorg.2019.102924
16. Xu L, Zhang Y, Zhang P, et al. Integrated metabolomics and network pharmacology Strategy-Driven active traditional Chinese medicine ingredients discovery for the alleviation of cisplatin nephrotoxicity. *Chem Res Toxicol*. 2019;32(12):2411–2421. doi:10.1021/acs.chemrestox.9b00180
17. Lee JH, Lim JY, Jo EH, et al. Chijabyukpi-Tang inhibits Pro-Inflammatory cytokines and chemokines via the Nrf2/HO-1 signaling pathway in TNF-alpha/IFN-gamma-Stimulated HaCaT cells and ameliorates 2,4-Dinitrochlorobenzene-Induced atopic Dermatitis-Like skin lesions in mice. *Front Pharmacol*. 2020;11:1018. doi:10.3389/fphar.2020.01018
18. Huang JH, Huang XH, Chen ZY, et al. Dose conversion among different animals and healthy volunteers in pharmacological trials. *Chin J Clin Pharmacol Ther*. 2004;9:1069–1072.
19. Fan HJ, Xie ZP, Lu ZW, et al. Anti-inflammatory and immune response regulation of Si-Ni-San in 2,4-dinitrochlorobenzene-induced atopic dermatitis-like skin dysfunction. *J Ethnopharmacol*. 2018;222:1–10. doi:10.1016/j.jep.2018.04.032
20. Li R, Guo C, Li Y, et al. Therapeutic targets and signaling mechanisms of vitamin C activity against sepsis: a bioinformatics study. *Brief Bioinform*. 2021;22(3):bbaa079. doi:10.1093/bib/bbaa079
21. Wang Z, Wang ZZ, Geliebter J, et al. Traditional Chinese medicine for food allergy and eczema. *Ann Allergy Asthma Immunol*. 2021;126(6):639–654. doi:10.1016/j.anai.2020.12.002
22. Gu L, Lu J, Li Q, et al. A network-based analysis of key pharmacological pathways of Andrographis paniculata acting on Alzheimer's disease and experimental validation. *J Ethnopharmacol*. 2020;251:112488. doi:10.1016/j.jep.2019.112488
23. Zhai B, Zhang N, Han X, et al. Molecular targets of beta-elemene, a herbal extract used in traditional Chinese medicine, and its potential role in cancer therapy: a review. *Biomed Pharmacother*. 2019;114:108812. doi:10.1016/j.biopha.2019.108812
24. Werfel T, Allam JP, Biedermann T, et al. Cellular and molecular immunologic mechanisms in patients with atopic dermatitis. *J Allergy Clin Immunol*. 2016;138(2):336–349. doi:10.1016/j.jaci.2016.06.010
25. Tsai YC, Chang HH, Chou SC, et al. Evaluation of the anti-atopic dermatitis effects of α-boswellic acid on Tnf-α/Ifn-γ-Stimulated HaCat Cells and DNCB-Induced BALB/c Mice. *Int J Mol Sci*. 2022;23(17):9863. doi:10.3390/ijms23179863
26. Wang J, Wang L, Lou GH, et al. Coptidis Rhizoma: a comprehensive review of its traditional uses, botany, phytochemistry, pharmacology and toxicology. *Pharm Biol*. 2019;57(1):193–225. doi:10.1080/13880209.2019.1577466
27. Wang XJ, Lin S, Kang HF, et al. The effect of RHIZOMA COPTIDIS and COPTIS CHINENSIS aqueous extract on radiation-induced skin injury in a rat model. *BMC Complement Altern Med*. 2013;13:105. doi:10.1186/1472-6882-13-105
28. Lee TK, Kang IJ, Kim B, et al. Experimental pretreatment with chlorogenic acid prevents transient Ischemia-Induced cognitive decline and neuronal damage in the hippocampus through anti-oxidative and anti-inflammatory effects. *Molecules*. 2020;25:16. doi:10.3390/molecules25163578
29. Ren Y, Sun-Waterhouse D, Ouyang F, et al. Apple phenolic extracts ameliorate lead-induced cognitive impairment and depression- and anxiety-like behavior in mice by abating oxidative stress, inflammation and apoptosis via the miR-22-3p/SIRT1 axis. *Food Funct*. 2022;13(5):2647–2661. doi:10.1039/d1fo03750a
30. Sun Z, Zeng J, Wang W, et al. Magnoflorine suppresses MAPK and NF-kappaB signaling to prevent inflammatory osteolysis induced by titanium particles in vivo and osteoclastogenesis via RANKL in vitro. *Front Pharmacol*. 2020;11:389. doi:10.3389/fphar.2020.00389

31. Xu T, Kuang T, Du H, et al. Magnoflorine: a review of its pharmacology, pharmacokinetics and toxicity. *Pharmacol Res*. 2020;152:104632. doi:10.1016/j.phrs.2020.104632
32. Yan B, Wang D, Dong S, et al. Palmatine inhibits TRIF-dependent NF-kappaB pathway against inflammation induced by LPS in goat endometrial epithelial cells. *Int Immunopharmacol*. 2017;45:194–200. doi:10.1016/j.intimp.2017.02.004
33. Long J, Song J, Zhong L, et al. Palmatine: a review of its pharmacology, toxicity and pharmacokinetics. *Biochimie*. 2019;162:176–184. doi:10.1016/j.biochi.2019.04.008
34. Qu L, Lin X, Liu C, et al. Atractylodin attenuates dextran sulfate Sodium-Induced colitis by alleviating gut microbiota dysbiosis and inhibiting inflammatory response through the MAPK pathway. *Front Pharmacol*. 2021;12:665376. doi:10.3389/fphar.2021.665376
35. Jacobi N, Seeboeck R, Hofmann E, et al. ErbB family signalling: a paradigm for oncogene addiction and personalized oncology. *Cancers*. 2017;9 (4). doi:10.3390/cancers9040033
36. Zhang Y, Li Y, Li H, et al. Clostridium difficile toxin B recombinant protein inhibits tumor growth and induces apoptosis through inhibiting Bcl-2 expression, triggering inflammatory responses and activating C-erbB-2 and Cox-2 expression in breast cancer mouse model. *Biomed Pharmacother*. 2018;101:391–398. doi:10.1016/j.biopha.2018.02.045
37. Shin JW, Lee HS, Na JI, et al. Resveratrol inhibits particulate Matter-Induced inflammatory responses in human keratinocytes. *Int J Mol Sci*. 2020;21(10):3446. doi:10.3390/ijms21103446
38. Mozolewski P, Moskot M, Jakobkiewicz-Banecka J, et al. Nonsteroidal anti-inflammatory drugs modulate cellular glycosaminoglycan synthesis by affecting EGFR and PI3K signaling pathways. *Sci Rep*. 2017;7:43154. doi:10.1038/srep43154
39. Pastore S, Mascia F, Mariani V, et al. The epidermal growth factor receptor system in skin repair and inflammation. *J Invest Dermatol*. 2008;128 (6):1365–1374. doi:10.1038/sj.jid.5701184
40. Mascia F, Mariani V, Girolomoni G, et al. Blockade of the EGF receptor induces a deranged chemokine expression in keratinocytes leading to enhanced skin inflammation. *Am J Pathol*. 2003;163(1):303–312. doi:10.1016/S0002-9440(10)63654-1
41. Saaf A, Pivarcsi A, Winge MC, et al. Characterization of EGFR and ErbB2 expression in atopic dermatitis patients. *Arch Dermatol Res*. 2012;304 (10):773–780. doi:10.1007/s00403-012-1242-4
42. Naeem AS, Zhu Y, Di WL, et al. AKT1-mediated Lamin A/C degradation is required for nuclear degradation and normal epidermal terminal differentiation. *Cell Death Differ*. 2015;22(12):2123–2132. doi:10.1038/cdd.2015.62
43. Gao C, Ding P, Yang L, et al. Oxymatrine sensitizes the HaCaT cells to the IFN-γ pathway and downregulates MDC, ICAM-1, and SOCS1 by activating p38, JNK, and AKT. *Inflammation*. 2018;41(2):606–613. doi:10.1007/s10753-017-0716-0
44. Wang W, Wang Y, Zou J, et al. The mechanism action of german chamomile (Matricaria recutita L) in the treatment of eczema: based on dose-effect weight coefficient network pharmacology. *Front Pharmacol*. 2021;12:706836. doi:10.3389/fphar.2021.706836
45. Hong S, Lee B, Kim JH, et al. Solanum nigrum Linne improves DNCBinduced atopic dermatitis like skin disease in BALB/c mice. *Mol Med Rep*. 2020;22(4):2878–2886. doi:10.3892/mmr.2020.11381
46. Duan W, Wong WS. Targeting mitogen-activated protein kinases for asthma. *Curr Drug Targets*. 2006;7(6):691–698. doi:10.2174/138945006777435353
47. Sur B, Kang S, Kim M, et al. Alleviation of atopic dermatitis lesions by a benzylideneacetophenone derivative via the MAPK signaling pathway. *Inflammation*. 2019;42(3):1093–1102. doi:10.1007/s10753-019-00971-w
48. Lorz LR, Kim MY, Cho JY. Medicinal potential of Panax ginseng and its ginsenosides in atopic dermatitis treatment. *J Ginseng Res*. 2020;44 (1):8–13. doi:10.1016/j.jgr.2018.12.012